Isı Bilimi ve Tekniği Dergisi, 33,1, 21-31, 2013
J. of Thermal Science and Technology

ISSN 1300-3615

NATURAL CONVECTION HEAT TRANSFER AND AIR FLOW IN RECTANGULAR ENCLOSURES WITH A WAVY WALL

Mesut TEKKALMAZ
Eskişehir Osmangazi University, Faculty of Engineering & Architecture, Metallurgical and Materials Engineering Department, 26480 Batı-Meşelik, Eskişehir,Turkey, tmesut@ogu.edu.tr

(Geliş Tarihi: 14. 09. 2010, Kabul Tarihi: 15. 07. 2011)

Abstract: A numerical investigation of laminar natural convection heat transfer and flow in two-dimensional wavy rectangular enclosures is presented. The enclosure is heated from the flat bottom wall and cooled from the wavy (undulated) top wall which is expressed by sinusoidal functions. The lateral walls are adiabatic. The numerical simulations were carried out by the commercially available CFD software—namely the FLUENT®. The steady-state continuity, Navier-Stokes and energy equations which are subjected to the Boussinesq approximation are solved using the SIMPLE algorithm. The convergence criteria for all equations are set to 10^{-5}. The Rayleigh numbers which are considered in the numerical simulations ranged from 5×10^4 to 10^7 while the value 0.7 was used for the Prandtl number of air. The enclosures with aspect ratios of L/H=1, 2, 4 and 8 were studied. The period, λ, for the sinusoidal functions imposed on the wavy wall was 1.5, 2.5 and 4.5 while the wave-amplitude was kept constant at a/H=0.1. The temperature field and the flow structure were analyzed for varying Rayleigh numbers. The aspect ratio, L/H, the number of undulations of the wavy wall, and the mean Nusselt numbers obtained from the bottom wall are computed and analyzed for each case.
Keywords: Natural convection, Laminar flow, Wavy enclosure, Heat transfer.

SİNUSOİDAL DUVARLI KAPALI DİKDÖRTGEN KUTULARDA HAVA AKIŞI VE DOĞAL TAŞINIM İLE ISI GEÇİŞİ

Özet: İki boyutlu sinusoidal duvarlı dikdörtgensel kapalı kutuda akış ve laminer doğal taşınım ile ısı geçişinin sayısal araştırması incelenmiştir. Kapalı kutunun, sinusoidal olarak değişen üst duvarı soğuk, alt duvarı ise sıcaktır. Düz duvarlar ise yalıtılmıştır. Sayısal çalışma, FLUENT® olarak bilinen, ticari CFD yazılım ile yapılmıştır. Boussinesq yaklaşımıyla beraber, sürekli rejimde süreklilik, taşınım ve enerji denklemleri, SIMPLE algoritması ile çözülmüştür. Bütün denklemlerde yakınsama kriteri 10^{-5} olarak alınmıştır. Sayısal çalışmada havanın Prandtl sayısı için 0.7 değeri kullanılırken, Rayleigh sayısı 5×10^4'den 10^7 değiştirilmiştir. Ortamın geometri oranı L/H=1, 2, 4 ve 8 olarak seçilmiştir. Sinusoidal duvarın genlik oranı a/H=0.1 olarak sabit tutulurken, sinusoidal fonksiyonun periyodu, λ, 1.5, 2.5 ve 4.5 olarak alınmıştır. Değişik Rayleigh sayısı için sıcaklık ve akış durumları analiz edilmiştir. Geometri oranı L/H, sinusoidal duvarın ondilin sayısına göre, alt duvardan elde edilen ortalama Nusselt sayıları her bir durum için hesaplanmış ve analiz edilmiştir.
Anahtar Kelimeler: Doğal taşınım, Laminer akış, Sinusoidal kapalı kutu, Isı geçişi.

NOMENCLATURE

a	Amplitude of waves [m]
A	Aspect ratio, L/H
g	Earth's gravitational acceleration [m/s^2]
H	Height of enclosure [m]
L	Length of enclosure [m]
Nu	Mean Nusselt number
P	Pressure [Pa]
Pr	Prandtl number [$=\nu/\alpha$]
Ra	Rayleigh number [$=g\beta H^3(T_h-T_c)/\alpha\nu$]
T	Temperature [K]
u,v	Fluid velocity components [m/s]
x,y	Coordinate axes [m]

Greeks

α	Thermal diffusivity [m/s^2]
β	Volumetric thermal expansion coefficient [K^{-1}]
ρ	Fluid density [kg/m^3]
ν	Kinematic viscosity [m/s^2]
λ	Wave period

Subscripts

c	cold
h	hot

INTRODUCTION

The natural convection in fluid filled rectangular enclosures has received considerable attention in recent years because of its relation to the thermal performance of engineering applications. The natural convection heat transfer from wavy surface is interest of several engineering applications such as cooling of electronic components and sealed electrical and/or electronic boxes, heating and cooling rooms, solar energy collector designs, heat exchanger designs so on. Thus, the characteristics of natural convection heat transfer are relatively important.

Yao (1983) theoretically studied the natural convection along a vertical wavy surface. He found that the local heat transfer rate is smaller than that of a flat plate case, and the heat transfer decreased with increasing wave-amplitude. The mean Nusselt number also showed the same trend. Saidi et al. (1987) presented numerical and experimental results for heat transfer and flow in a sinusoidal cavity. They reported that the total heat exchange between the wavy wall of the cavity and the fluid was reduced due to the presence of vortices. They indicated that the vortices played the role of a thermal screen, which created a large region of uniform temperature at the bottom of the cavity. Bhavnani and Bergles (1991) obtained local free heat transfer coefficients from a vertical wavy wall and observed a decrease in heat transfer from the wavy wall. Kumari et al. (1997) studied the natural convection boundary layer flow of non-Newtonian fluids along a vertical wavy surface. Rahman (2001) obtained data on natural mass convection from vertical wavy. Mahmud et al. (2002) presented numerical solutions of natural convection heat transfer inside an enclosure bounded by two isothermal wavy walls and two adiabatic lateral walls. They observed that aspect ratio is the most important parameter for the heat and fluid flow. They also found that for a constant Grashof number, the heat transfer is higher at low aspect ratios. Mahmud and Islam (2003) also solved the laminar natural convection and entropy generation inside an inclined enclosure bounded by two isothermal wavy walls. They reported that the lower the surface waviness, the higher the heat transfer for a particular angular position is. Adjlout et al. (2002) reported a numerical study of a hot wavy wall in an inclined differentially heated square cavity. Tests, for one and three undulations, were performed for different inclination angles, different amplitudes and Rayleigh numbers. The local heat transfer was also wavy and the mean Nusselt number decreased in comparison to the bare square cavity. Jang et al. (2003) solved numerically the natural convection heat and mass transfer along a vertical wavy surface by using Prandtl's transposition theorem and investigated the effect of irregular surfaces on characteristics of natural convection heat and mass transfer. Das and Mahmud (2003) analyzed the natural convection heat transfer inside both the bottom and the top wavy isothermal enclosures. They indicated that, only at low Grashof numbers, the heat transfer rate increased when the amplitude wave length ratio changed near zero values. Dalal and Das (2005) carried out a numerical solution to investigate the heat transfer from an inclined right wavy wall enclosure subjected to spatially varying temperature boundary condition. Yao (2009) investigated the natural convection along a vertical complex wavy surface. The numerical results showed that the enhanced heat transfer rate depended on the ratio of amplitude and wavelength of a surface. Varol and Oztop (2006) analyzed the natural convection in a shallow wavy enclosure. Their results showed that heat transfer increased with the decreasing non-dimensional wave length and increased with the increasing aspect ratio and the Rayleigh number. The authors also investigated the natural convection in inclined wavy and flat-plate solar collectors (Varol and Oztop, 2008).

The purpose of the present paper is to study heat transfer and fluid flow characteristics of a rectangular enclosure which is heated from the bottom flat wall (Benard convection) and cooled from the undulated (wavy) top wall. The undulated wall was expressed by appropriate sinusoidal functions that yield one, two and four undulations. For the fluid flow and heat transfer analysis, the local and mean Nusselt numbers for various Rayleigh numbers and aspect ratios are evaluated along the hot wall, and the isotherms and streamlines are depicted.

MATHEMATICAL FORMULATION

The problem under consideration is a two-dimensional rectangular enclosure with a wavy top wall. The schematic of the geometry and coordinate system is depicted in Figure 1. The enclosure of height H and length L has a wavy-top wall (cold) and flat (hot) bottom wall. The walls are kept at uniform constant temperatures while the side walls are flat and adiabatic. The enclosure is filled with air (Pr=0.7). The Rayleigh numbers considered in this study ranged from 5×10^4 to 10^7. The enclosure aspect ratios considered in the study are L/H=1, 2, 4 and 8. The period of sinusoidal function imposed on the top-wavy wall is λ=1.5 (one undulation, Case 1), λ=2.5 (two undulations, Case 2), and λ=4.5 (four undulations, Case 3) while the wave-amplitude was kept constant at a/H=0.1.

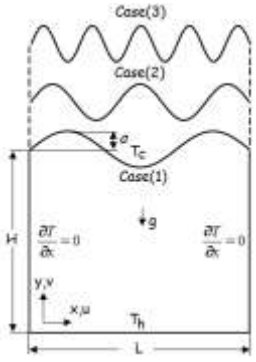

Figure 1. Schematic of the problem and the coordinate system.

The continuity, momentum and energy equations for two-dimensional cartesian coordinate system are solved

using the Boussinesq approximation. The governing equations are defined as follows:

The continuity equation

$$\frac{\partial u}{\partial x}+\frac{\partial v}{\partial y}=0 \tag{1}$$

The momentum equations

$$u\frac{\partial u}{\partial x}+v\frac{\partial v}{\partial y}=-\frac{1}{\rho}\frac{\partial P}{\partial x}+\nu\left(\frac{\partial^2 u}{\partial x^2}+\frac{\partial^2 v}{\partial y^2}\right) \tag{2}$$

$$u\frac{\partial u}{\partial x}+v\frac{\partial v}{\partial y}=-\frac{1}{\rho}\frac{\partial P}{\partial y}+\nu\left(\frac{\partial^2 u}{\partial x^2}+\frac{\partial^2 v}{\partial y^2}\right)+g\beta\left(T-T_\infty\right) \tag{3}$$

and the energy equation

$$u\frac{\partial T}{\partial x}+v\frac{\partial T}{\partial y}=\alpha\left(\frac{\partial^2 T}{\partial x^2}+\frac{\partial^2 T}{\partial y^2}\right) \tag{4}$$

Equations (1)-(4) are subject to the following boundary conditions:

At the bottom wall, $T=T_h$,

At the top wall, $T=T_c$, (5)

On side walls, $\partial T/\partial x=0$,

All walls are solid and impermeable; that is, $u=v=0$.

The wavy top horizontal wall is expressed by the following sinusoidal function:

$$f(x)=H+a\sin\left[\frac{2\pi\lambda x}{A}\right] \tag{6}$$

where a is the amplitude, A is the aspect ratio of the enclosure and λ is the wave-period.

Non-dimensional parameters such as Rayleigh and Prandtl numbers are defined as

$$Ra=\frac{g\beta H^3(T_h-T_c)}{\nu\alpha},\qquad \mathrm{Pr}=\frac{\nu}{\alpha} \tag{7}$$

The mean Nusselt number is computed for the bottom hot-wall

$$\overline{\mathrm{Nu}}=-\frac{1}{L}\int_{x=0}^{L}\left[\frac{\partial T}{\partial y}\right]_{y=0}dx \tag{8}$$

Equations (1)-(4) are solved with non-uniform grids condensed near the walls. In the differencing scheme of the transport terms the "Second Order Upwind" and SIMPLE was adopted as the solution algorithm.

For the verification of the results obtained with FLUENT, an air filled square cavity, which is heated and cooled from the lateral walls, is considered. This problem has been studied extensively using various methods and plenty of solutions exist in the literature. In Table 1, the mean Nusselt number computed using 100×100 and 200×200 non-uniform grid configurations are compared with other works (Vahl Davis, 1983; Comini et al., 1995; Bilgen, 2005). Additionally, the accuracy of the FLUENT software in natural convection and CFD is well established in numerous studies (Mahir and Altaç, 2008; Zhoa et al., 2005; Kasier et al., 2004).

Table 1. Computer code results in comparison with other works.

Ra	Mean Nusselt Number				
				Fluent	
	Vahl Davis (1983)	Comini et al. (1995)	Bilgen (2005)	100x100 (11433 nodes)	200x200 (45500 nodes)
10^4	2.243		2.245	2.244	2.245
10^5	4.519	4.503	4.521	4.521	4.521
10^6	8.799	8.825	8.800	8.834	8.827
10^7		16.533	16.629	16.653	16.543

Table 2. Grid Sensitivity table.

Ra	Mean Nusselt Number		
	Number of nodes		
	27,600	81,718	162,290
10^5	4.586	4.583	4.583
5×10^5	6.760	6.744	6.742
10^6	7.956	7.925	7.921
5×10^6	11.613	11.471	11.452
10^7	13.548	13.422	13.395

In this study, the grid sensitivity analysis and code verification was based on the convergence of the mean Nusselt number. For instance, in Table 2, the convergence of the mean Nusselt number for increasing Rayleigh numbers and increasing number of grids is depicted for A=8 of Case (2). In this study, non-uniform grids near the walls, where sharp velocity and temperature gradients are expected, were employed. The grid structure, in general, yielded about 80 to 162 thousand nodes depending on the aspect ratio of the enclosure. In terms of the sufficiency of the grid structure, a two-significant-digit-accurate converged value ($Ra<5\times10^6$) for mean Nusselt number was assumed to be adequate.

RESULTS AND DISCUSSIONS

In this study, an air filled (Pr=0.7) enclosure with a wavy top-surface and the aspect ratios of A=1, 2, 4 and 8 are considered. Numerical simulations are carried out for the following Rayleigh numbers: 5×10^4, 10^5, 5×10^5, 10^6, 5×10^6 and 10^7.

Figure 2 depicts the isotherms and streamlines for A=1, 2, 4 and 8 and for $Ra=5\times10^5$ of one undulation enclosures—Case (1). In Figure 2 (a) and (b), for A=1 and A=2, the streamlines and isotherms are in similar

form. The clockwise flow is mainly unicellular encompassing the whole domain; however, a weak counter-clockwise roll is observed in the northwest cavity of A=1 enclosure. In Figure 2 (c) and (d), in enclosures with A=4 and A=8, four and six rolls are observed, respectively. From left to the right, the structure of the rolls switches from the counter-clockwise to clockwise direction. This leads hydrodynamic boundary layers to thin out where the rolls become tangent to the bottom wall. Similarly the isotherms are squeezed about the same locations due to the flow structure. Thus, the local Nusselt number profiles are affected due to the various formations of thermal boundary layers accompanied by an increase in the number of rolls. This results in thinner boundary layers along the hot wall yielding an increase in the number of peaks in the local Nusselt number profiles.

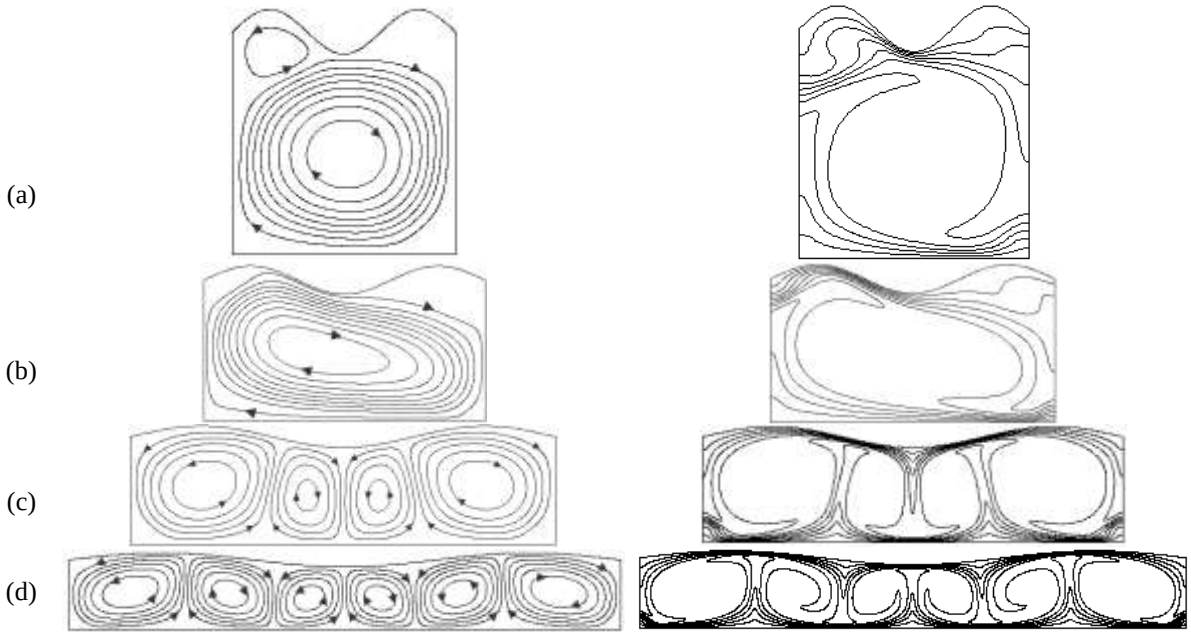

Figure 2. Isotherms (right) and streamlines (left) for Case (1) and $Ra=5\times10^5$ (a) A=1, (b) A=2, (c) A=4, (d) A=8.

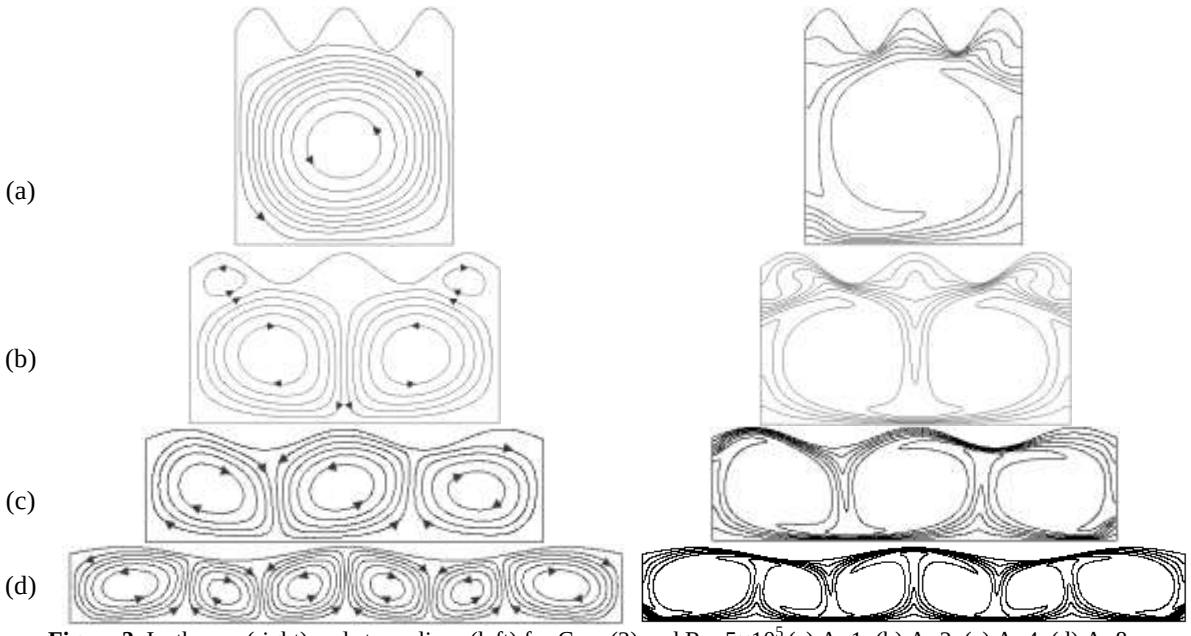

Figure 3. Isotherms (right) and streamlines (left) for Case (2) and $Ra=5\times10^5$ (a) A=1, (b) A=2, (c) A=4, (d) A=8.

Figure 3, the isotherms and the streamlines for two-undulation enclosures (Case 2) and for $Ra=5\times10^5$ with aspect ratios of A=1, 2, 4 and 8 are depicted. In Figure 3 (a), for A=1, the flow circulation extends out to encompass the enclosure and it rotates in the counter-clock-wise direction. In Figure 3 (b), for A=2, two strong counter-rotating cells are established. Two accompanying small and weak rolls at the corners of the top-wavy wall are symmetrical with respect to the mid plane. In Figure 3 (c), for A=4, three cells with two rising hot plumes and two downward cold plumes are formed in the enclosure. The local Nusselt number profiles become maximum where the cold plume touches the hot wall as the thermal boundary layers are

squeezed towards the wall. In Figure 3 (d), six rolls are formed in the enclosure and the local Nusselt number profile is observed to have four distinct-peaks.

Figure 4 depicts the isotherms and streamlines for A=1, 2, 4 and 8 and for Ra=5×10^5 of four-undulation enclosures—Case (3). In Figure 4 (a), for A=1, the flow is unicellular encompassing the whole domain, and flow is in the clockwise direction. The flow region seems to be restricted by the horizontal line defined with minimum points of the waves. For A=2, in Figure 4 (b), two strong counter-rotating cells (clockwise left roll and counter-clockwise right roll), along with two small and very weak opposite rolls at the corners of the cold wavy wall, are observed. In Figure 4 (c), for A=4, three rolls are observed in the domain; from left to the right the direction of the rolls switch between clockwise to counter-clock wise. As a result of this structure, two hot and two cold plumes are formed in the enclosure. In Figure 4 (d), for A=8, eight rolls are observed in the enclosure, since four downward cold plume touches the hot wall, four peaks are observed in the local Nusselt profile.

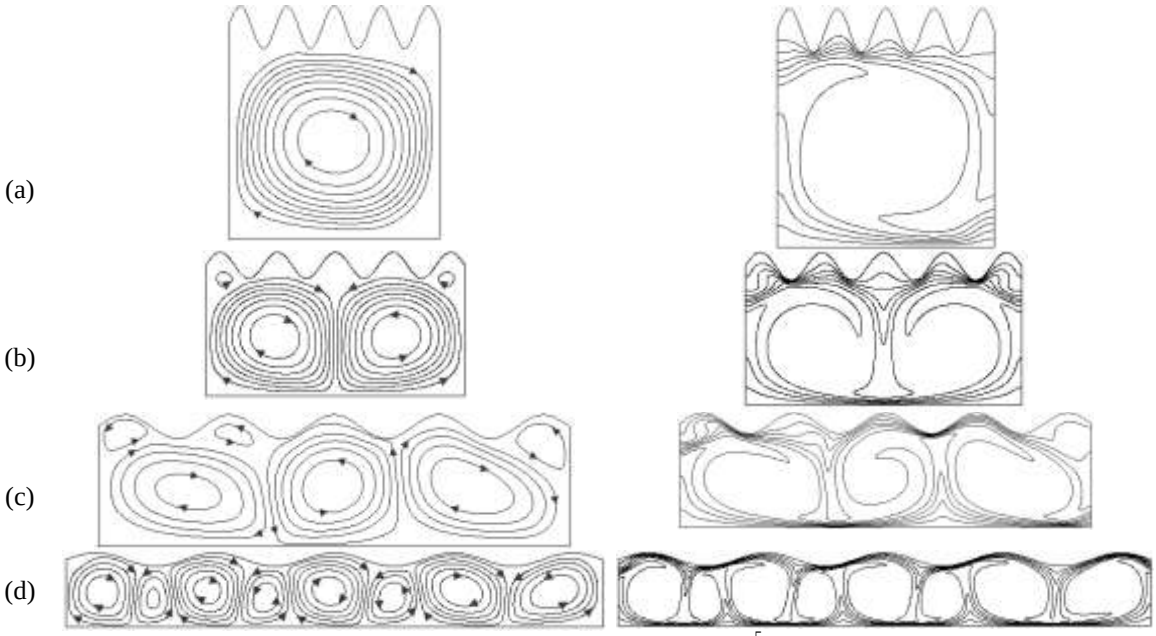

Figure 4. Isotherms (right) and streamlines (left) for Case (3) and Ra=5×10^5 (a) A=1, (b) A=2, (c) A=4, (d) A=8.

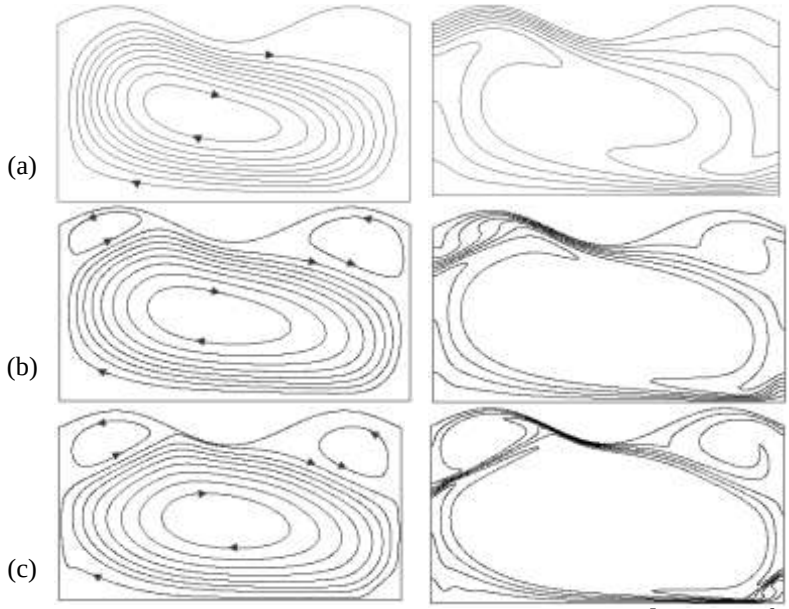

Figure 5. Isotherms (right) and streamlines (left) for Case (1) and A=2, (a) Ra=10^5, (b) Ra=10^6 and (c) Ra=10^7.

In Figure 5, the isotherms and streamlines are depicted for Rayleigh numbers of 10^5, 10^6, 10^7 of A=2 and one undulation. For all Rayleigh values, a single clockwise-rotating cell dominates the flow within the enclosure, but at the corners of the cold wavy wall in Figure 5 (b) and (c), at Ra=10^6 and Ra=10^7, two small weak rolls rotating in opposite directions are observed. As the

Rayleigh numbers increase, the roll gains strength and the thermal boundary layers thin out further.

For A=2, Figure 6 depicts the isotherms and streamlines for Rayleigh number of 10^5, 10^6, 10^7 of two-undulation wall, Case (2). For all Rayleigh numbers, two counter-rotating cells are established within the enclosure, and in Figure 6 (b) and (c), for Ra=10^6 and Ra=10^7, two small as well as weak rolls at the corners of cold wavy wall are observed. With increasing Rayleigh number, these small rolls expand out as they get stronger. The two hot plumes rise along the adiabatic lateral walls while a downward cold plume touches the hot bottom wall where thermal boundary layer is getting thinner and longer with increasing Ra values. In Figure 7, the isotherms and streamlines are depicted for Rayleigh numbers of 10^5, 10^6, 10^7 of Case (3) and A=2. For all Rayleigh values, two strong counter-rotating rolls are formed within the enclosure. As in the previous cases, for Ra=10^6 and Ra=10^7, two small-weak rolls at the corners of cold wavy wall are observed—Figure 7(b) and (c). These rolls gain further strength as the Rayleigh number is increased. It should be noted that the hot and cold plumes become thinner for increasing Rayleigh number as the thermal boundary layers are also squeezed at the tip of the cold plume where the local Nusselt number is the maximum.

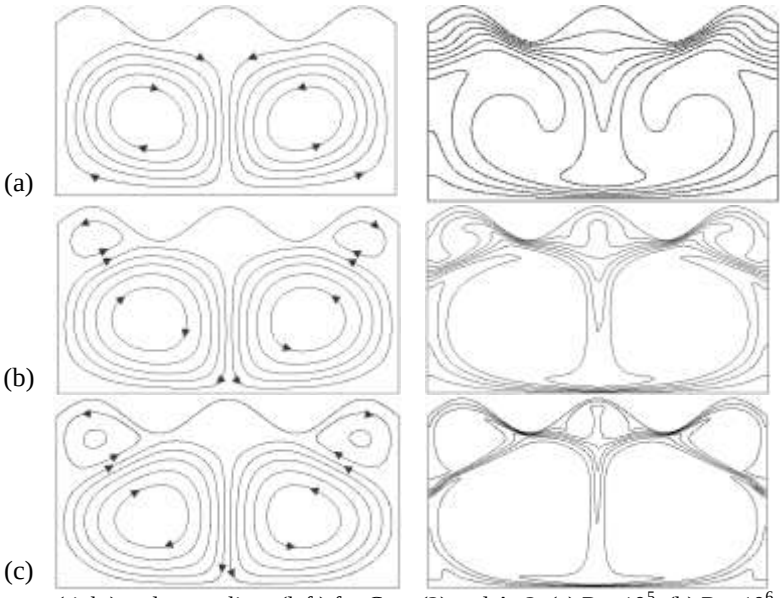

Figure 6. Isotherms (right) and streamlines (left) for Case (2) and A=2, (a) Ra=10^5, (b) Ra=10^6 and (c) Ra=10^7.

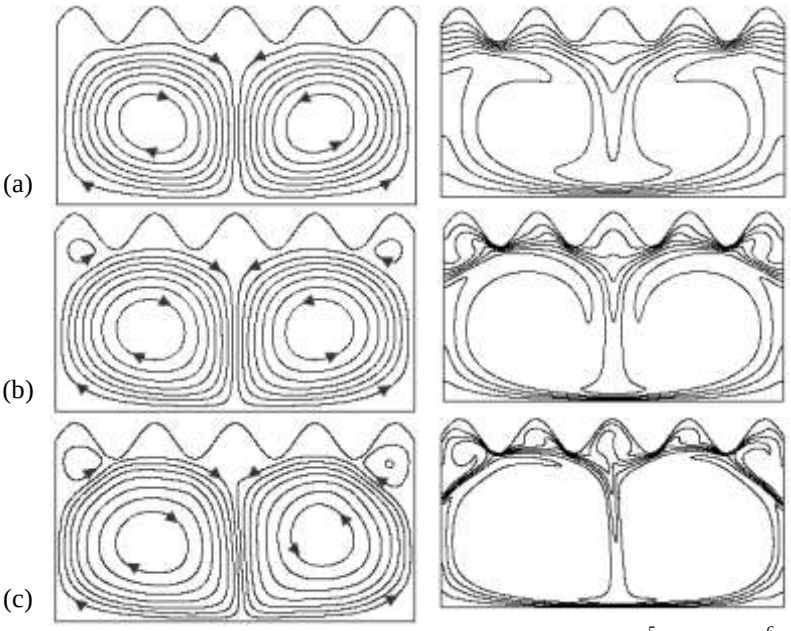

Figure 7. Isotherms (right) and streamlines (left) for Case (3) and A=2, (a) Ra=10^5, (b) Ra=10^6 and (c) Ra=10^7.

In Figure 8, the isotherms and streamlines are depicted for Rayleigh numbers of 5×10^4, 5×10^5, 5×10^6 of Case 2 (wavy wall with two-undulations) and A=4. In Figure 8 (a), for $Ra=5\times10^4$, four cells with rising three hot plumes and two downward cold plumes are formed in the domain. The first roll at the left side of the enclosure is always in clockwise direction. The proceeding rolls switch directions. In Figure 8 (b) and (c), as the three rolls are formed in the enclosure in a similar fashion, two hot and cold plumes are observed due to expanding stronger rolls are noticed and for increasing Rayleigh values thinning plumes are observed. Similarly with increasing Rayleigh number, the thermal boundary layer on the hot bottom wall thins out where the circular rolls become tangent to the hot wall which also correspond to the tip of the cold plumes.

In Figure 9, the isotherms and streamlines are depicted for Rayleigh numbers of 5×10^4, 5×10^5, 5×10^6 of Case (3) and A=8. In Figure 9 (a), for $Ra=5\times10^4$, eight cells with rising five hot plumes and four downward cold plumes are observed in the enclosure. For $Ra=5\times10^4$ and $Ra=5\times10^5$, in Figure 9 (b) and (c), the number of rolls are reduced to seven due to expanding more energetic rolls within the domain. As the Rayleigh number increases, the number of rolls in the enclosure changes and the rolls expand out while the number of peaks in the local Nusselt number remains unaffected.

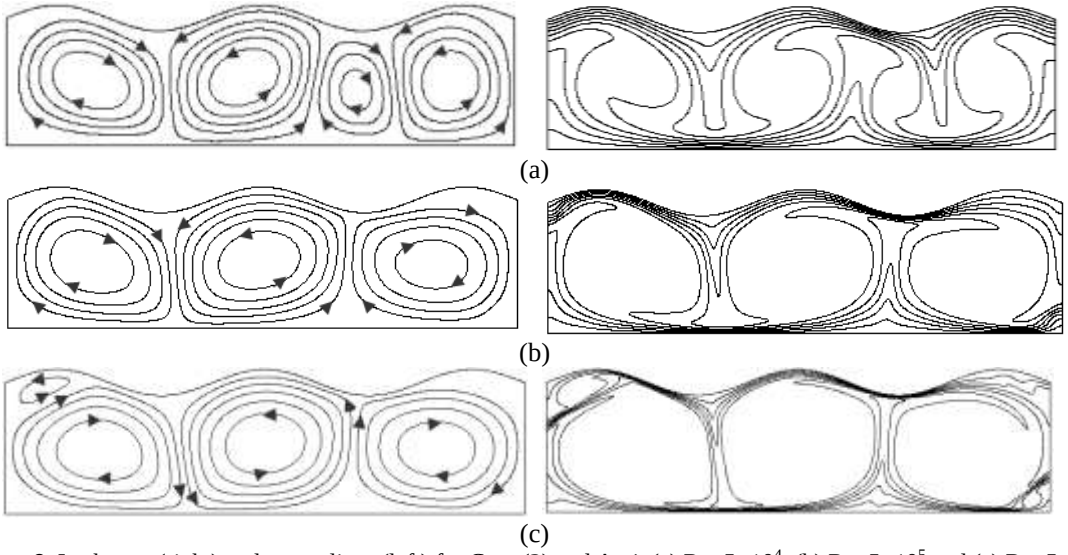

Figure 8. Isotherms (right) and streamlines (left) for Case (2) and A=4, (a) $Ra=5\times10^4$, (b) $Ra=5\times10^5$ and (c) $Ra=5\times10^6$.

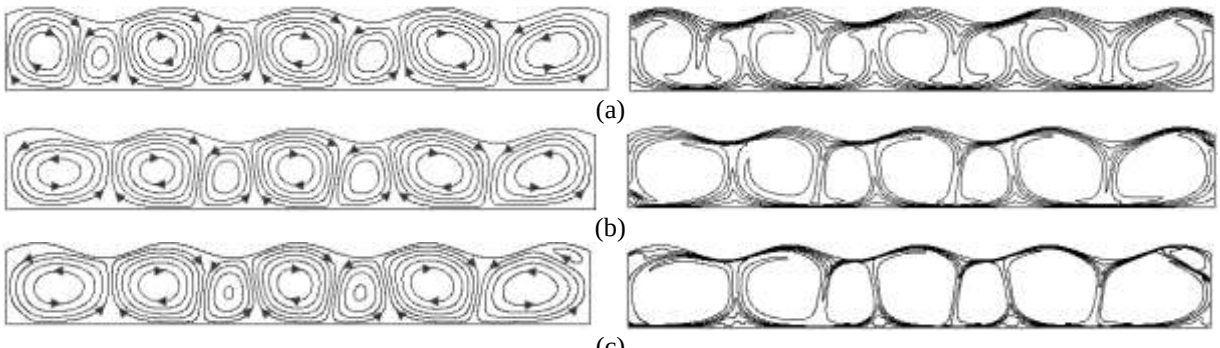

Figure 9. Isotherms (right) and streamlines (left) for Case (3) and A=8, (a) $Ra=10^5$, (b) $Ra=10^6$ and (c) $Ra=10^7$.

In Figure 10 (a), the variation the local Nusselt number is depicted for A=1 and Case (1). The local Nusselt number is higher near the right wall (Figure 2a), but as the Rayleigh number increases, for $Ra>5\times10^4$ the peak becomes more distinct, and it shifts towards the middle of the bottom wall where the thermal boundaries are clearly thin. In Figure 10 (b), the variation the local Nusselt number is depicted for A=1 and Case (2), the local Nusselt number profile peaks near the left wall due to the established flow structure (Figure 3a). Similarly, with increasing Rayleigh number, the peak moves towards the center of the bottom wall while its magnitude increases. In Figure 10 (c), the variation the local Nusselt number is depicted for A=1 and Case (3); for $Ra>5\times10^5$, the peak of the local Nusselt number is near the right wall. For $Ra=5\times10^6$, the peak also shifts slightly towards to the centre of the enclosure due to the flow pattern.

In Figure 11 (a), the variation the local Nusselt number is depicted for A=2 and Case (1). For all the Rayleigh values which numerical simulations were performed, the peak of the local Nusselt number appeared near the right wall where strong clockwise circulations skim over the bottom wall; thereby, affecting the thermal boundary formation and its thickness (Figure 2b) along

this surface. In Figure 11 (b), the variation the local Nusselt number is depicted for A=2 and Case (2). The flow structure and isotherms were given in Figure 3. The two counter rotating rolls yield symmetrical streamlines and isotherms with respect to the enclosure centerline; thus yielding the maximum local Nusselt number at the center of the bottom wall. In Figure 11 (c), the variation the local Nusselt number profile is depicted for A=2 and Case (3). For all the cases and the Rayleigh numbers, the maximum of local Nusselt number is at the center due to the established symmetrical flow pattern (Figure 4b).

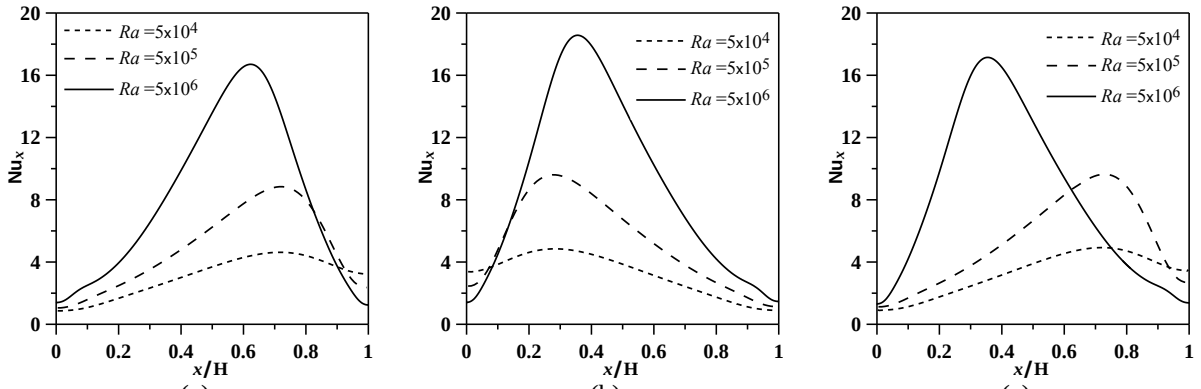

Figure 10. Variation of local Nusselt number along hot wall for A=1, (a) Case (1), (b) Case (2) and (c) Case (3).

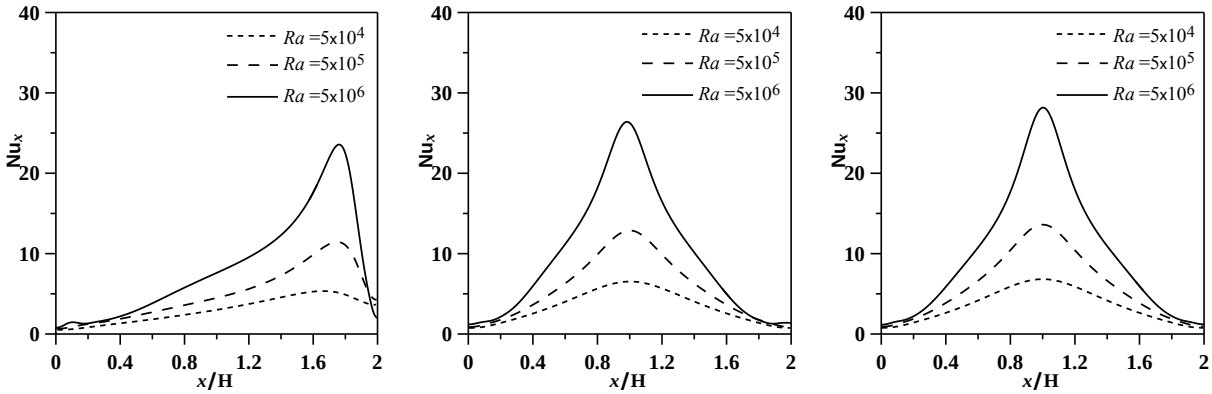

Figure 11. Variation of local Nusselt number along hot wall for A=2, (a) Case (1), (b) Case (2) and (c) Case (3).

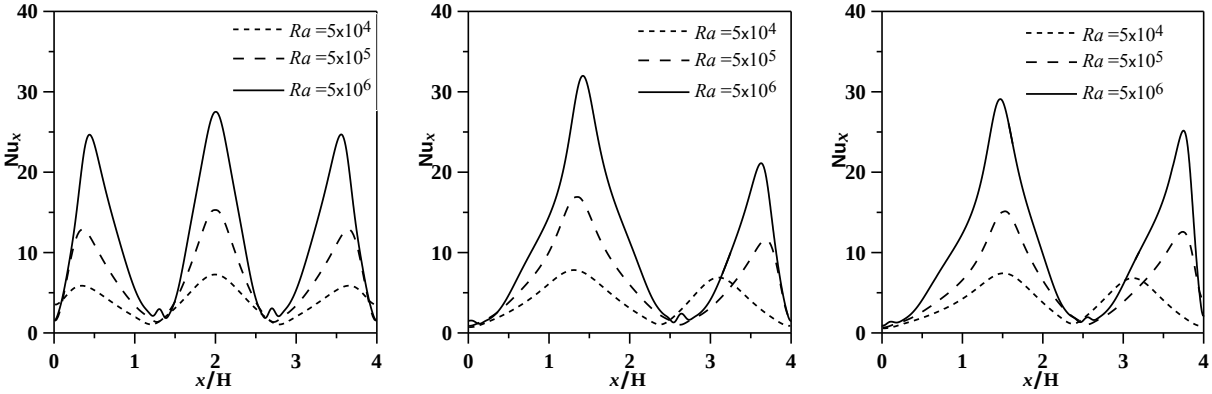

Figure 12. Variation of local Nusselt number along hot wall for A=4, (a) Case (1), (b) Case (2) and (c) Case (3).

In Figure 12 (a), the variation the local Nusselt number profile is depicted for A=4 and Case (1). For all Rayleigh numbers, three peaks, symmetrical with respect to the centerline, are observed. These peaks correspond to the thinnest thermal boundary layer thickness locations: the middle peak is caused by downward cold plume while the other two peaks correspond to tangents of the rolls (Figure 2c). In Figure 12 (b), the variation the local Nusselt number is depicted for A=4 and Case (2). The local Nusselt number has two peaks due to the flow pattern (Figure 3c) where thermal boundary layers become the thinnest due to downward cold plumes. In Figure 12 (c), the variation the local Nusselt number is depicted for A=4

and Case (3). Since the number of undulations is increased, two detaching hot plumes and two downward cold plumes are observed leading to two peaks in the local Nusselt number profile as in the case Figure 12(b). As the Rayleigh number is increased, the locations of the peaks are consistent with the trend of the thermal boundary layer thicknesses.

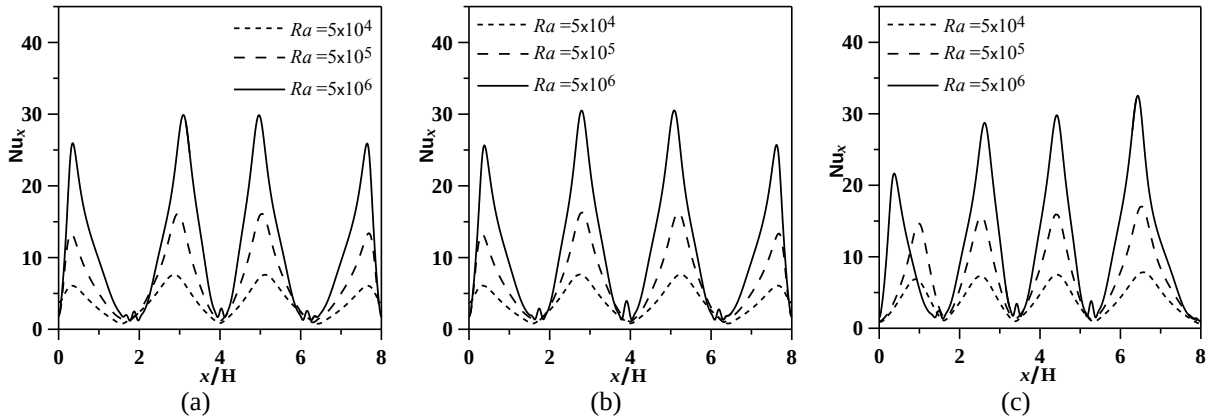

Figure 13. Variation of local Nusselt number along hot wall for A=8, (a) Case (1), (b) Case (2) and (c) Case (3).

In Figure 13, the variation the local Nusselt number profile for A=8 and (a) Case(1), (b) Case (2) and (c) Case (3) is given. For all the wavy-wall cases and the Rayleigh numbers, four local Nusselt number peaks are observed where the downward cold plumes touch the hot bottom wall. As the Rayleigh number is increased, due to the strengthening and outward expanding rolls, the corresponding thermal boundary layers are getting thinner and the local Nusselt number increases.

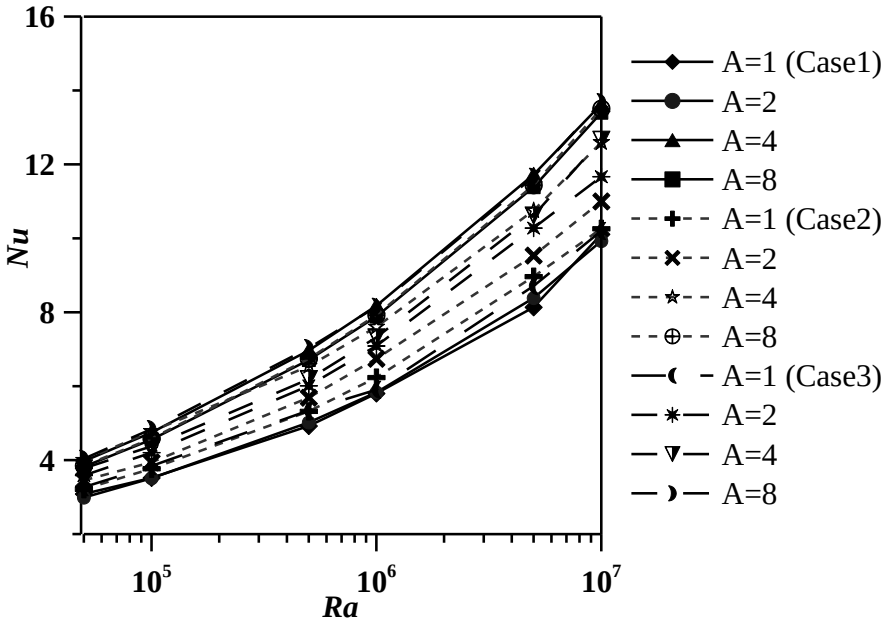

Figure 14. The mean Nu number variation for all Ra numbers.

Figure 14 depicts, for all the cases, the mean Nusselt number as a function of Rayleigh number and aspect ratio. The mean Nusselt number increases with increasing Rayleigh number and aspect ratio. As the Rayleigh number increases, for Case (1), A=1 and A=2, the mean Nusselt values are almost identical; the maximum difference between the two cases is about 3.17%. For $Ra=10^6$ and A=1, the mean Nusselt value increases by 0.49%, 40.9% and %35.9%, respectively for A=2, 4 and 8. For Case(2) and $Ra=10^6$, mean Nusselt number of A=1 compares with other aspect ratios cases as 8.14%, 21.92% and 27.04% respectively for A=2, 4 and 8. For Case(2), the maximum mean Nusselt values were obtained for $Ra>10^5$ of A=8. In Case(3), $Ra=10^6$ and A=1, the increase in the mean Nusselt number with respect to other aspect ratio enclosures is 20.07%, 23.97% and 38.01% respectively for A=2, 4 and 8. When all the simulated cases are considered, with respect to the increase in Rayleigh number, the highest rates were obtained in A=4 of Case(1) and in A=8 of Case(3). As the number of undulation is increased, for the same Rayleigh values, the mean Nusselt values increase for A=1, Case(1) and Case(2); for Case(3) it increases up to $Ra<5\times10^5$ then

decreases. For all the cases of A=2 and A=8, the mean Nusselt number increases while it decreases for A=4 cases. The largest increase is observed for A=2 as the number of undulations increases. For Ra=10^6 and A=2 of Case(1), the increase with respect to the mean Nusselt values are 15.62% and 21.58% respectively for Case (2) and Case (3).

CONCLUSION

Laminar natural convection heat transfer and air flow in enclosures with a top wavy cold wall was numerically studied. The numerical simulations were performed for the Rayleigh numbers ranging from 5×10^4 to 10^7 and for the aspect ratios of *A*=1, 2, 4 and 8. The wavy wall with one, two and four undulations were considered. The hot (bottom)-wall-averaged mean Nusselt numbers were computed and reported as a function of Rayleigh number, undulation numbers (wave-period) and the aspect ratio.

The study concludes the following:

- For a constant aspect ratio A, the mean Nusselt number increases with increasing Rayleigh number.
- For a constant Rayleigh number, the mean Nusselt number increases with increasing aspect ratio but for A>2 this increase in minimal.
- The number of undulations influences the flow patterns within the enclosure; however, the mean Nusselt numbers resulting for the hot wall are not significantly affected especially at low Rayleigh values.
- The minimum mean Nusselt number is obtained at Case (1) for A=1 and A=2, the maximum mean Nusselt number is obtained for A=4 Case (1) and A=8 Case (3).

REFERENCES

Adjlout, L., Imine, O., Azzi, A., and Belkadi M., Laminar natural convection in an inclined cavity with a wavy wall, *International Journal of Heat and Mass Transfer*, 45, 2141-2152, 2002.

Bhavnani, S. H. and Bergles, A. E., Natural convection heat transfer from sinusoidal wavy surfaces, *Heat and Mass Transfer*, 26, 341-349, 1991.

Bilgen, E., Natural convection in cavities with a thin fin on the hot wall, *International Journal of Heat and Mass Transfer*, 48, 3493-3505, 2005.

Comini, G., Cortella, G., and Manzan M., A stream function-vorticity-based finite element formulation for laminar convection, *Numerical Heat Transfer, Part B*, 28, 1-22, 1995.

Dalal, A. and Das, M.K., Laminar natural convection in an inclined complicated cavity with spatially variable wall temperate, *International Journal of Heat and Mass Transfer*, 48, 3833-3854, 2005.

Das, P. K. and Mahmud, S., Numerical investigation of natural convection inside a wavy enclosure, *International Journal of Thermal Science*, 42, 397-406, 2003.

Jang, J. H., Yan, W. M. and Liu, H. C., Natural convection heat and mass transfer along a vertical wavy surface, *International Journal of Heat and Mass Transfer*, 46, 1075-1083, 2003.

Kaiser, A. S., Zamora, B. and Viedma, A., Correlation for Nusselt number in natural convection in vertical convergent channels at uniform wall temperature by a numerical investigation, *International Journal of Heat and Fluid Flow*, 25, 671-682, 2004.

Kumari, M., Pop, I. and Takhar, H. S., Free-convection boundary-layer flow of a non-Newtonian fluid along a vertical wavy surface, *International Journal of Heat and Fluid Flow*, 18, 625-631, 1997.

Mahir, N. and Altaç, Z., Numerical investigation of convection heat transfer in unsteady flow past two cylinders in tandem arrangements, *International Journal of Heat and Fluid Flow*, 29,1309-1318, 2008.

Mahmud, S., Das, P. K., Hyder, N. and Islam, A. K. M. S., Free convection heat transfer in an enclosure with vertical wavy walls, *International Journal of Thermal Science*, 41, 440-446, 2002.

Mahmud, S. and Islam, A. K. M. S., Laminar free convection and entropy generation inside wavy enclosure, *International Journal of Thermal Science*, 42, 1003-1012, 2003.

Rahman, S. U., Natural convection along vertical wavy surfaces: an experimental study, *Chemical Engineering Journal*, 84, 587-591, 2001.

Saidi, C., Legay, F. and Pruent, B., Laminar flow past a sinusoidal cavity, *International Journal of Heat and Mass Transfer*, 30, 649-660, 1987.

Vahl Davis, G., D., Natural convection of air in a square cavity: benchmark numerical solution, *International Journal for Numerical Methods in Fluids*, 3, 249-264, 1983

Varol, Y. and Oztop, H. F., Free convection in a shallow wavy enclosure, *International Communications in Heat and Mass Transfer*, 33, 764-771, 2006.

Varol, Y. and Oztop, H. F., A comparative numerical study on natural convection in inclined wavy and flat-plate solar collectors, *Building and Environment*, 43, 1535-1544, 2008.

Yao, L. S., Natural convection along a vertical wavy surface, *Journal of Heat Transfer*, 105, 465-468, 1983.

Yao, L. S., Natural convection along a vertical complex wavy surface, *International Journal of Heat and Mass Transfer*, 49, 281-286, 2009.

Zhoa, B., Vanta, S. P. and Thomas, B. G., Numerical study of flow and heat transfer in molten flux layer, *International Journal of Heat and Fluid Flow*, 26, 105-118, 2005.

Mesut TEKKALMAZ, He was born in Eskişehir-Turkey in 1972. He graduated from Department of Mechanical Engineering of Eskişehir Anadolu University in 1994. He received the degree of MSc and PhD from Department of Mechanical Engineering of Eskişehir Osmangazi University in 1996 and 2003, respectively. He is assistant professor of Metallurgical and Materials Engineering Department in Eskişehir Osmangazi University.